Research Article

Payam Shafie*, Alain DeChamplain, Julien Lepine

Theoretical investigation of hydrogen-rich fuel production through ammonia decomposition

https://doi.org/10.1515/chem-2024-0020
received February 22, 2024; accepted April 3, 2024

Abstract: Considering the challenges related to hydrogen storage and transportation which hinder its widespread adoption, ammonia has emerged as a carbon-free carrier for hydrogen due to several advantages such as simple inexpensive storage. But, due to some limitations related to net ammonia combustion, the suggestion is to store hydrogen in the form of ammonia and convert it into hydrogen-rich fuel before utilization in different applications like engines and turbines. Therefore, in this article, a comprehensive thermodynamic analysis of hydrogen-rich fuel production via ammonia decomposition is conducted utilizing Aspen Plus V.12, to assess the impact of operating parameters on key criteria such as conversion rate (CR) and enthalpy of reaction, to establish the maximum level of efficiency of the process. The results show that at a specific temperature, the CR of ammonia decreases as the pressure rises so that the CR of more than 50% occurred at temperatures of 427 and 513 K for pressures of 1 and 10 bar, respectively. Moreover, the adiabatic flame temperature of hydrogen-rich fuel is investigated so that increasing the molar percentage of hydrogen from 0 to 50 leads to an increase in the maximum adiabatic flame temperature from 2,079 to 2,216 K.

Keywords: ammonia decomposition, hydrogen, thermodynamics, equilibrium

*** Corresponding author: Payam Shafie**, Department of Mechanical Engineering, Laval University, Quebec, Canada,
e-mail: Payam.shafie.1@ulaval.ca
Alain DeChamplain: Department of Mechanical Engineering, Laval University, Quebec, Canada
Julien Lepine: Department of Operations and Decision Systems, Laval University, Quebec, Canada

1 Introduction

CO_2 is the most effective greenhouse gas in terms of elevating atmospheric temperature so that its concentration currently stands at about 417 parts per million (ppm) by volume and experienced a consistent annual increase of over 2 ppm for the 11th consecutive year in 2022 [1]. To reduce CO_2 emissions, effective utilization of alternate carbon-free fuels has become significantly important [2]. Hydrogen (H_2) is one of the most important carbon-free fuels due to its high performance in multiple purposes so its global demand from 2000 to 2021 increased from 50 to 94 Mt [3].

The problem of storage and transportation of hydrogen is one of the most significant challenges for its feasible utilization as a fuel. Hydrogen gas molecules are smaller than those of any other gas, allowing it to permeate through many materials typically regarded as airtight or impermeable to other gases. Although hydrogen has the highest heating value by mass among all fuels (LHV = 119.6 MJ/kg), it has a very low heating value by volume at standard conditions, which is one-third of methane gas [4]. It is typically stored in two main ways, one of which involves storing it as a highly compressed gas, reaching pressures of up to 700 bar at a temperature of 298 K. In addition, hydrogen can be stored in its liquid form, which demands much lower temperatures, specifically 20 K at 1 bar. Achieving liquefaction in this manner would necessitate a substantial energy input of approximately 11.6 MJ/kg [5]. Such storage systems are energy-demanding and extremely expensive, so the ways and means to handle it economically and safely are a challenge that needs to be solved.

Ammonia (NH_3) has been recognized as a promising carbon-free alternative for supplying hydrogen since it has a high gravimetric hydrogen density of 17.8 wt%, suitable LHV of 18.8 MJ/kg, and a volumetric energy of 11.3 MJ/L in its liquid form [6]. In contrast to the challenges linked with storing and transporting hydrogen, ammonia can be liquefied under mild conditions and stored in a simple, cost-effective pressure vessel since the vapour pressure of ammonia at room temperature is 9.2 bar [7]. Moreover, the existing

infrastructure for ammonia production, storage, and transportation is well-established and the global production capacity of ammonia is expected to expand from around 236 million tons in 2021 to nearly 290 million tons by 2030 [8]. Ammonia also benefits from a lower boil-off rate, approximately 0.025 vol%/day, in comparison with hydrogen which can be up to 5 %vol/day [9]. Moreover, 1 mol of ammonia contains 1.5 mol of hydrogen so that 108 kg of hydrogen is embedded in 1 m^3 liquid ammonia at 293 K, which is four times higher than the most advanced hydrogen storage systems, such as metal hydrides [10]. Ammonia is highly resistant to auto-ignition which makes it safe to be transported so that its auto-ignition temperature is 924 K compared to hydrogen at 858 K [11].

Despite the numerous advantages provided by ammonia usage, there are certain limitations especially related to net ammonia combustion as a fuel. Ammonia has a low laminar flame speed (S_L = 15 cm/s at atmospheric conditions) compared to other fuels such as diesel at about 87 cm/s [12], which leads to low burning efficiency in engines. Its combustion includes three specific emissions that relate to safety, health, and climate: NH_3 unburned or slip, NO_x, and N_2O [13]. Therefore, one of the most practical ways to enhance the flame speed of ammonia combustion and reduce NH_3 slip and N_2O is to use combustion promoters.

Considering the advantages of ammonia as a hydrogen carrier and due to the poor combustion performance of ammonia fuel, it is proposed to carry hydrogen in the ammonia-bound form and, immediately before use, to decompose a part of the ammonia into H_2 as a promoter. This H_2-rich fuel leads to a simpler fuel storage system and reduces the need for additional modifications in different applications such as engines [14,15]. Gill et al. [16] investigated co-fuelling a diesel engine in three different modes including only NH_3, dissociated NH_3 (H_2-rich fuel), and pure H_2 as the second fuel. They showed that by substituting only 3% of the air intake with H_2-rich gas, diesel consumption, and CO_2 emissions decreased by 15%. Yang et al. [17] studied the effect of varying H_2/NH_3 ratios (10 to 90% energy fraction) on different parameters of a single-cylinder diesel engine. The results demonstrated that when the hydrogen blending ratio reached 30% compared to 0, the unburned NH_3 was eliminated and N_2O significantly decreased by 97%.

Given the mentioned advantages of H_2-rich gas as a fuel, the usage of an ammonia decomposition system becomes important since it can produce CO_x and sulphur-free stream of hydrogen, and unconverted ammonia can be easily reduced to safe levels in one-step adsorption [18]. Thermal decomposition or catalytic cracking is the most common technique used for the generation of hydrogen from ammonia [19]. To ensure the efficient use of raw materials and energy inputs for the ammonia decomposition system, thermodynamic analysis enables to optimize reactor designs, catalyst type, and operating conditions.

In this article, to assess how varying operational parameters can impact different key performance criteria of the ammonia decomposition reaction, the technical analysis of hydrogen-rich gas production via ammonia decomposition is performed using Aspen Plus V.12 considering ideal-gas equation of state and idealized Gibbs reactor. Using the thermodynamic principles allows us to provide results for ultimate levels of conversion rate (CR) and required energy. These limiting levels can serve as a basis for the optimum design of different parts of ammonia decomposition systems, evaluating related experimental studies and developing more efficient systems of hydrogen utilization in different applications including internal combustion engines, gas turbines, and industrial furnaces. Moreover, the adiabatic flame temperature (T_{ad}) is investigated for different ammonia/hydrogen mixtures and various equivalence ratios so that such analysis is useful for researchers and professionals concerned with safety and the optimization of combustion efficiency for different hydrogen-based fuel applications.

2 Methodology

The decomposition of ammonia is reverse to that of its synthesis, as a typical single-step endothermic process with an enthalpy change of 46.19 kJ/mol which is much lower than electrolysis at 237.1 kJ/mol [20,21]:

$$2NH_{3(g)} \rightarrow N_{2(g)} + 3H_{2(g)}. \quad (1)$$

In this article, the thermodynamic analysis of hydrogen-rich gas production through ammonia decomposition is performed using Aspen Plus V.12 considering the ideal-gas equation of state. Such thermodynamic analysis will be a guideline for assessing the performance of actual catalytic reactors due to the importance of evaluating the maximum CR and energy consumption of the decomposition system at different operating conditions. Therefore, ammonia decomposition evaluation is conducted considering the idealized Gibbs reactor. The reactor determines the decomposition products by employing the Gibbs free energy minimization method. Different criteria are considered, especially ammonia CR [22] (equation (2)), hydrogen-rich gas energy ratio (ER) [23] (equation (3)), and enthalpy variation.

$$\mathrm{CR} = \frac{\dot{m}_{\mathrm{NH_{3,in}}} - \dot{m}_{\mathrm{NH_{3,out}}}}{\dot{m}_{\mathrm{NH_{3,in}}}}, \tag{2}$$

$$\mathrm{ER} = \frac{\dot{m}_{\mathrm{H_2}}\mathrm{LHV}_{\mathrm{H_2}} + \dot{m}_{\mathrm{NH_{3,out}}}\mathrm{LHV}_{\mathrm{NH_{3,out}}}}{\dot{m}_{\mathrm{NH_{3,in}}}\mathrm{LHV}_{\mathrm{NH_{3,in}}}}, \tag{3}$$

where $\dot{m}_{\mathrm{NH_{3,in}}}$ and $\dot{m}_{\mathrm{NH_{3,out}}}$ are ammonia mass flow rate at the inlet and outlet of the reactor, and LHV is the lower heating value of the fuel.

In the Gibbs free energy minimization technique, the system is thermodynamically favourable when its total Gibbs free energy reaches its minimum value and its differential equals zero for given temperature (T) and pressure (P) [24]:

$$\mathrm{d}G = 0. \tag{4}$$

The Gibbs free energy (G) is a thermodynamic extensive property which combines the enthalpy (H) and the entropy (S) of a system and is defined by equation (5):

$$G = H - \mathrm{TS}. \tag{5}$$

The differential change of the Gibbs function of a pure substance is:

$$\mathrm{d}G = V\mathrm{d}P - S\mathrm{d}T, \tag{6}$$

where V is the volume. For a system consisting of different species, the total Gibbs function is a function of two independent intensive properties as well as the molar composition which can be expressed as equation (7), and its differential is based on equations (8) and (9) [25]:

$$G = G(P, T, n_1, n_2, \ldots, n_i), \tag{7}$$

$$\mathrm{d}G = V\mathrm{d}P - S\mathrm{d}T + \sum_i \left(\frac{\partial G}{\partial n_i}\right)_{P,T,n_j} \mathrm{d}n_i, \tag{8}$$

$$\mathrm{d}G = V\mathrm{d}P - S\mathrm{d}T + \sum_i \mu_i \mathrm{d}n_i, \tag{9}$$

where n_i is the number of moles of species present in the system and μ_i is the chemical potential of species "i," which is the change in the Gibbs function of the mixture in a specified phase when a unit amount of component (i) in the same phase is added as pressure, temperature, and the amounts of all other components are held constant. Equation (8) can be mathematically integrated into a process in which the size of the system is increased by adding systems with the same intensive properties, all intensive properties remain constant, and all extensive properties increase proportionally. Hence, $\mathrm{d}T = 0$, $\mathrm{d}P = 0$, $\mathrm{d}\mu_i = 0$ in such a process, showing that equation (9) can readily be integrated from ($G = 0$, $n_i = 0$) to (G, n_i) so that the total Gibbs free energy of the ammonia decomposition process can be calculated as a sum of the chemical potential of all components [26].

$$G = \sum \mu_i n_i. \tag{10}$$

Therefore, equation (11) shows the Gibbs function differential for the system at a given temperature and pressure in chemical equilibrium.

$$\mathrm{d}G = \sum \mu_i \mathrm{d}n_i. \tag{11}$$

Moreover, the chemical potential of each of the species of an ideal gaseous mixture is given by equation (12).

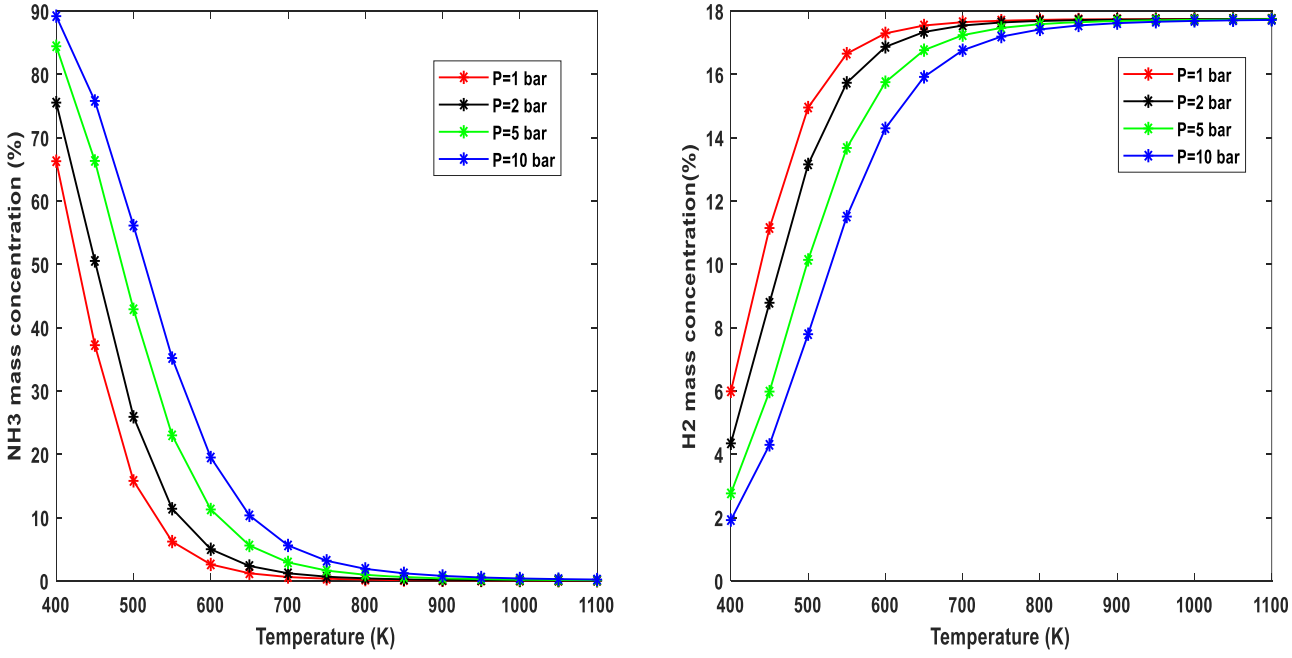

Figure 1: NH_3 and H_2 mass concentrations at different pressures and temperatures.

$$\mu_i(T, P_i) = \mu_i(T, P) + R_u T \ln\left(\frac{P_i}{P}\right), \tag{12}$$

where $\mu_i(T, P)$ is the chemical potential of the pure substance i when it exists alone at total mixture pressure and temperature, which is equivalent to the Gibbs function since the chemical potential and the Gibbs function are identical for pure substances. So, the objective function of minimization in Aspen Plus could be formulated as follows:

$$G(T, P, n_i) = \sum n_i \left(\mu_i(T, P) + R_u T \ln\left(\frac{P_i}{P}\right)\right). \tag{13}$$

3 Results and discussion

Figure 1 shows the equilibrium mass concentration of ammonia and hydrogen product as a function of temperature ranging from 400 to 1,100 K at different pressures from 1 to 10 bar. This range of pressure is selected since it covers the proper range in different applications such as dual-fuel engines, fuel cells, and even hydrogen production considering the utilization of a separation technique like pressure swing adsorption. The results reveal that higher temperatures at constant pressure, or lower pressures at constant temperature lead to a higher percentage of the produced hydrogen. Due to the importance of the partial decomposition of ammonia in dual-fuel applications, it is worth mentioning that the mass concentration of hydrogen can reach a maximum of 17.8% at temperatures of 600 and 650 K when the pressure is 1 and 2 bar, respectively. Regarding the effect of pressure, at a constant temperature of 600 K, ammonia mass concentration is 2.5% at P = 1 bar, while this amount for P = 10 bar increases to 19.5%.

The equilibrium constant, K_{eq}, expresses the relation between products and reactants of a reaction at equilibrium with respect to a specific unit. The equilibrium constant expression is derived from the law of mass action so that it can be expressed by equation (14) in terms of equilibrium composition for ammonia decomposition [26].

$$K_{eq} = \frac{N_{H_2}^{1.5} N_{N_2}^{0.5}}{N_{NH_3}} \left(\frac{P}{N_t}\right), \tag{14}$$

where P is the total pressure and N_t is the total number of moles present in the reaction.

Figure 2 shows the variation of K_{eq} based on temperature. The results obtained from Aspen Plus are validated by comparing them with the equilibrium constant for ammonia synthesis derived from Temkin and Pyzhev's formula (equation (15)) [27]. The strong agreement between the two indicates

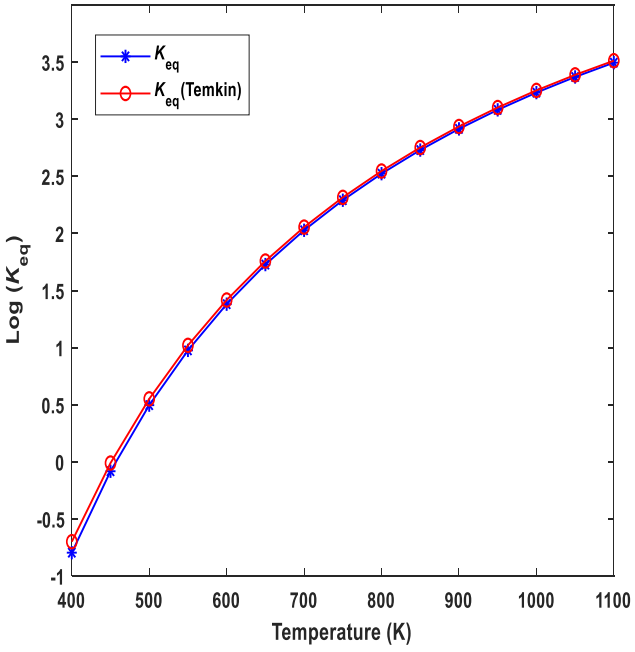

Figure 2: Validation of equilibrium constant as a function of temperature for ammonia decomposition.

the accuracy of Aspen Plus results, supported by the reciprocal relationship between the equilibrium constants for decomposition and synthesis.

$$\log_{10} K_{eq} = 2.6899 + 2001.6 \times T^{-1} + 1.848863 \times 10^{-7} \times T^{-2} - 2.691122 \log_{10} T - 5.519265 \times 10^{-5} \times T. \tag{15}$$

Since the reaction is endothermic, the increase in temperature provides the necessary energy to overcome the activation energy barrier required for the reaction to occur. Therefore, at higher temperatures, the decomposition of ammonia is favoured, leading to an increase in the value of K_{eq}. The larger the K_{eq} value, the more the ammonia decomposition reaction will tend toward the right and thus to completion.

The thermodynamic equilibrium represents the maximum conversion that can be achieved, regardless of the catalyst and reaction rates so it depends only on temperature, pressure, and inflow composition. According to equation (1), Figure 3 (left) shows the effect of pressure and temperature on the ammonia CR. The results reveal that as the temperature increases, particularly beyond 700 K, the influence of pressure on ammonia conversion diminishes and it is more than 95%. Furthermore, at a specific temperature, the conversion of ammonia decreases as the pressure rises. It is noticeable that CR of more than 50% occurred at temperatures of about 427, 450, 484, and 513 K for pressures of

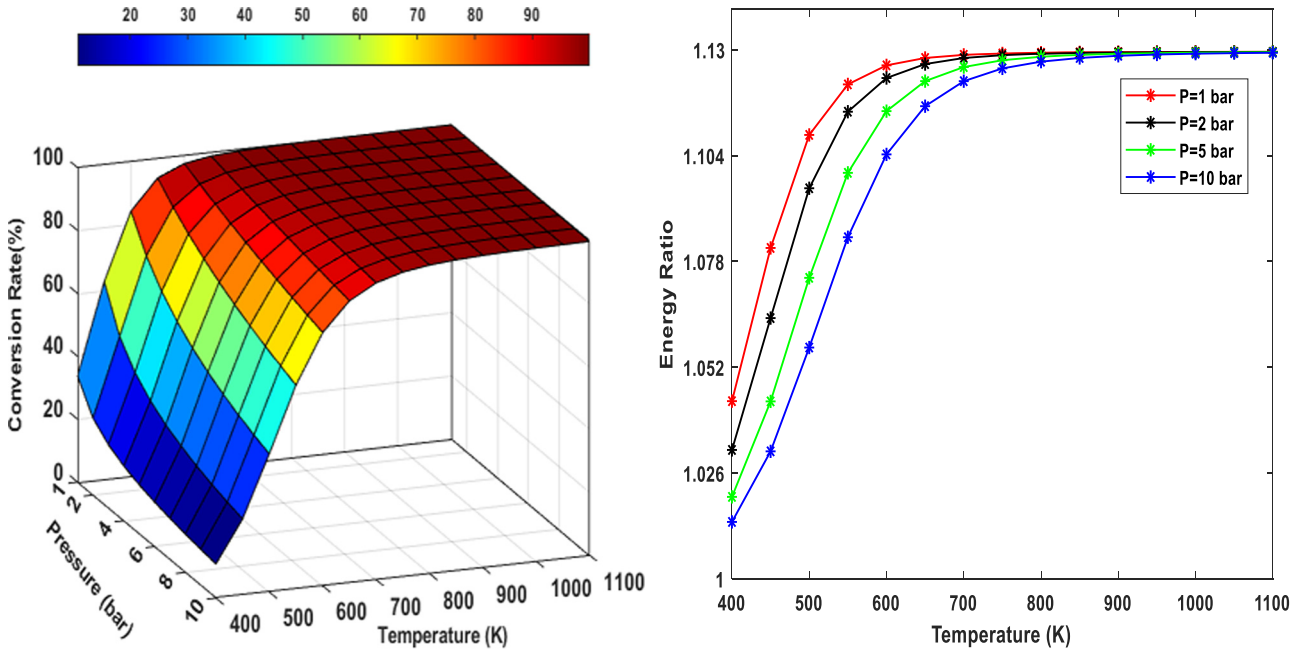

Figure 3: Variation of NH_3 CR (left) and ER by temperature and pressure (right).

1, 2, 5, and 10 bar respectively. Moreover, Considering the LHV of ammonia and hydrogen as per equation (2), Figure 3 (right) indicates the ER of the H_2-rich gas to ammonia inlet at different temperatures and pressures. The results reveal that the maximum achievable ER is 1.13, which can occur at temperatures higher than 700 K regardless of pressure. Regarding the effect of temperature, at P = 1 bar, an ER of 1.08 and 1.12 are achievable for temperatures of 450 and 550 K.

The equilibrium constant for the reaction can also be related to the standard Gibbs free energy change, $\Delta G°$ which is related to the standard pressure, of the reaction at a given temperature as equation (16) [28].

$$\ln K = \frac{-\Delta G°}{R_u T}, \tag{16}$$

where R_u is the gas constant at 8.314 J/mol K. Moreover, $\Delta H°$ and $\Delta S°$ determine the magnitude of $\Delta G°$:

$$\Delta G^0 = \Delta H^0 - T\Delta S^0. \tag{17}$$

Figure 4 demonstrates the variation of ΔG^0, ΔH^0, and $T\Delta S^0$ as a function of temperature for the ammonia decomposition so that considering the standard temperature, the validity of the simulation can be proved since standard Gibbs free energy for ammonia decomposition should be +16.5 kJ/mol [29]. The reaction is thermodynamically favourable at temperatures more than 453 K in the forward direction by reaching negative standard Gibbs free energy. Figure 4 also shows that as the temperature increases, the entropy change becomes more significant, which results in a wider range of $T\Delta S^0$ values. The ΔS is positive because one molecule of NH_3 decomposes into more molecules of gas (N_2 and H_2), increasing the disorder of the system. The enthalpy changes from 44.85 to 55.60 kJ/mol which is generally less sensitive to temperature variations, and its

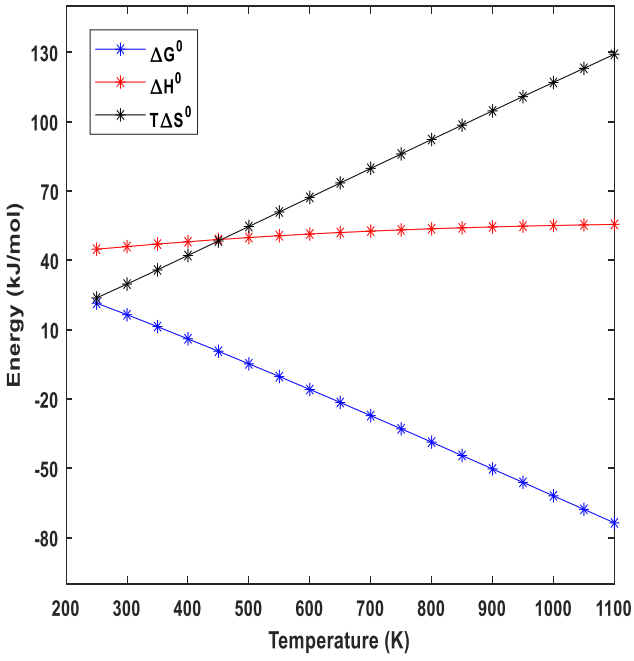

Figure 4: Variation of $\Delta G°$, $\Delta H°$, and $T\Delta S°$ as a function of temperature for ammonia decomposition.

profile agrees with endothermic reactions. At lower temperatures, the positive ΔH^0 term dominates, making ΔG positive and the reaction non-spontaneous. At higher temperatures, the positive $T\Delta S^0$ term becomes more significant, and the reaction becomes spontaneous.

The enthalpy change of the reaction (ΔH_r) is the difference between the enthalpy of the products at a specified state (H_P) and the enthalpy of the reactants at the same state (H_R) considering equations (18)–(20) [30].

$$\Delta H_r = H_P - H_R, \tag{18}$$

$$H_P = \sum N_p(\bar{h}_f^0 + \bar{h} - \bar{h}^0)_P, \tag{19}$$

$$H_R = \sum N_R(\bar{h}_f^0 + \bar{h} - \bar{h}^0)_R, \tag{20}$$

where $\bar{h}_f^0$, $\bar{h}$, and $\bar{h}^0$ are the enthalpy of formation, the sensible enthalpy at the specified state and the sensible enthalpy at the standard reference state respectively. Figure 5 illustrates the effect of pressure and temperature on the enthalpy of the ammonia decomposition reaction so that as temperature rises, the reaction enthalpy also rises at a specified pressure, while the pressure increasing leads to a decrease in the reaction enthalpy due to Le Chatelier's Principle and the endothermic nature of the reaction. The effect of temperature on the enthalpy change is more pronounced for the temperature lower than 700 K compared to higher temperatures so that ΔH is between 3,000 and 3,254 kJ/kg for temperatures higher than 700 K and it remains relatively constant after 950 K.

Considering the definition of ER and CR, and based on the results related to Figure 3, it can be concluded that for any pressure and temperature, there is a linear relationship between ER and CR (equation (21)), which is shown by the blue line in Figure 6.

$$\mathrm{ER} = 1 + 0.13\mathrm{CR}. \tag{21}$$

Moreover, the LHV of the reactor outlet mixture by considering N_2 as the dilution component is calculated using equation (22), and the results are shown in Figure 6 in comparison with the LHV of a conventional fuel such as diesel, which is significant for dual-fuel engines in different applications such as maritime and vehicular transportation. The LHV of the gas mixture ($\mathrm{LHV_{mix}}$) is calculated for all different pressures, and the results reveal that it can be only considered as a function of CR. According to Figure 6, the LHV of the H_2-rich gas rises as the CR increases. At CR ≈ 63%, $\mathrm{LHV_{mix}}$ reaches equivalence with diesel fuel so that based on Figure 2, for pressures of 1, 2, 5, and 10 bar, temperatures of about 450, 470, 512, and 544 K are required, respectively, for such a conversion.

$$\mathrm{LHV_{mix}} = \frac{\dot{m}_{H_2}\mathrm{LHV}_{H_2} + \dot{m}_{NH_{3,out}}\mathrm{LHV}_{NH_{3,out}}}{\dot{m}_{H_2} + \dot{m}_{NH_{3,out}}}. \tag{22}$$

Combustion is the most important step in all kinds of applications of H_2-rich gas including gas turbines, internal combustion engines, and furnaces. Therefore, the study of adiabatic flame temperature, as the maximum temperature of the combustion gas that can be reached by the

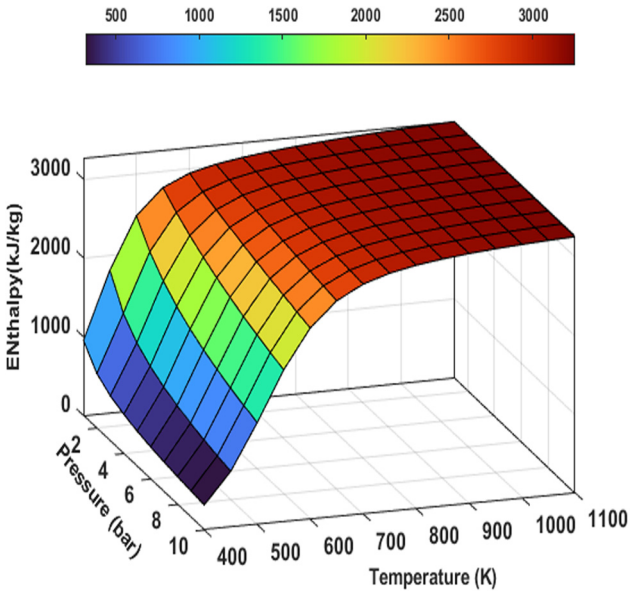

Figure 5: Enthalpy of ammonia decomposition as a function of temperature and pressure.

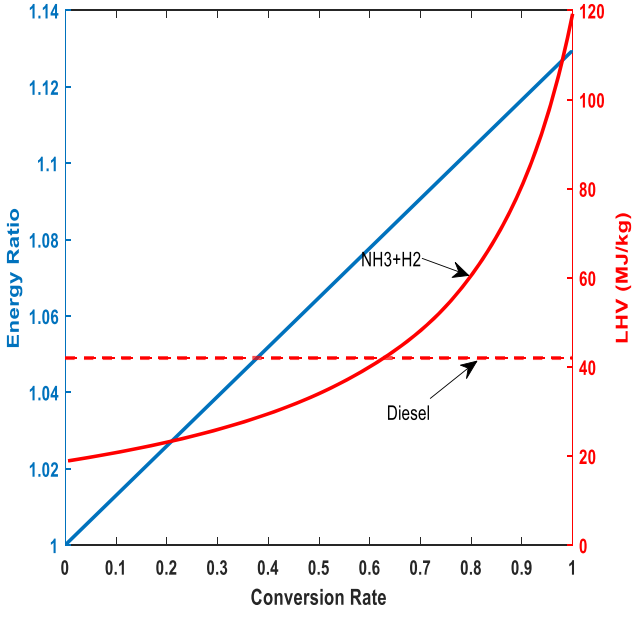

Figure 6: Variation of ER and lower heating value of the H2-rich gas by CR.

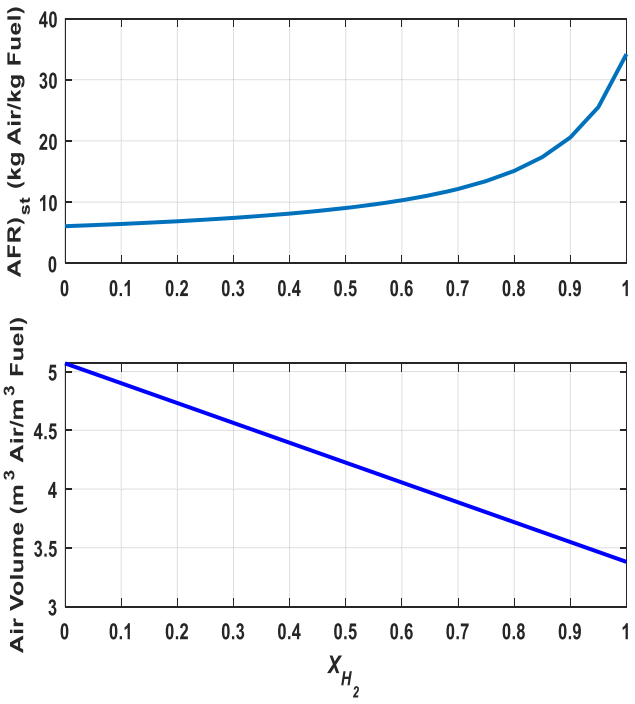

Figure 7: Variation of stoichiometric air/fuel ratio and theoretical air volume for the H_2-rich gas.

combustion reaction under no heat loss to the surroundings in the adiabatic condition (equation (23) [26]), is of vital importance since the higher flame temperature may be preferable for practical applications of H_2-rich gas combustion.

$$\sum N_R(\bar{h}_f^0 + \bar{h} - \bar{h}^0)_R = \sum N_p(\bar{h}_f^0 + \bar{h} - \bar{h}^0)_P. \quad (23)$$

Combustion simulation is carried out by using an adiabatic constant-pressure Gibbs reactor model in Aspen Plus V.12. This simulation is processed for 21 mixtures (different hydrogen mole fractions in 0.05 increments) with the equivalence ratio (φ) covering from 0.4 to 1.6 (equation (24)). First, the stoichiometric air/fuel ratio at each molar percentage of hydrogen (x_{H2}) is determined using equation (25), so that Figure 7 illustrates that by increasing the hydrogen percentage in H_2-rich gas, stoichiometric air to fuel ratio rises from 6.1 to 34.1 kg_{Air}/kg_{Fuel}. This ratio for conventional fuels like diesel and methane is about 14.5 and 17.2 kg_{Air}/kg_{Fuel}, respectively [4]. Moreover, theoretical air volume shows that less air volume is required for combustion as the hydrogen content of the mixture increases, thus reducing the volume of the combustion products.

$$\varphi = \frac{(m_{fuel}/m_{air})_{actual}}{(m_{fuel}/m_{air})_{st}}, \quad (24)$$

$$(1-x)NH_3 + xH_2 + \left(\frac{3-x}{4}\right)(O_2 + 3.76N_2) \rightarrow 3.76\left(\frac{3-x}{4}\right)N_2 + \left(\frac{3-x}{2}\right)H_2O. \quad (25)$$

According to the above-mentioned points, Figure 8 (left) shows the adiabatic flame temperature based on considering different exhaust species including H_2, NH_3, O_2, N_2, H_2O, N_2O, NO, and NO_2. It can be concluded that increasing the molar percentage of hydrogen from 0 to 50% and 100%

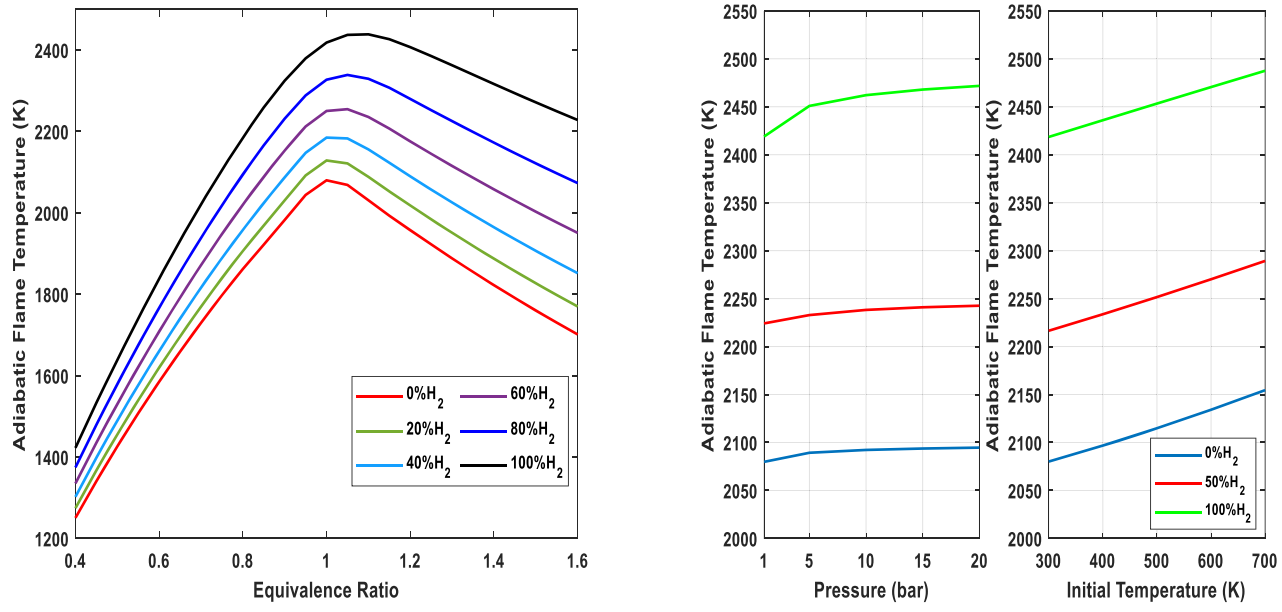

Figure 8: Adiabatic flame temperature (T = 298 K, P = 1 bar, left) and effect of pressure and initial temperature on the adiabatic flame temperature of H_2-rich gas (right).

in the fuel mixture leads to the increase of maximum adiabatic flame temperature from 2,079 to 2,216 K and 2,438 K. It is worth mentioning that the maximum adiabatic flame temperature for diesel is 2,573 K [31]. When the equivalence ratio falls below one (lean mixture), there is an excess of air extracting heat from the reaction. On the other hand, when the equivalence ratio is greater than one (rich mixture), there is a higher concentration of unburnt fuel that consumes energy, but this is less than the heat taken away by air during lean combustion. Moreover, by increasing the hydrogen content to more than 80%, the maximum values of the adiabatic flame temperature of mixtures occur slightly on the rich side of the fuel equivalence ratio (off-stoichiometric peaking of adiabatic flame temperature [32]). This is because the products of rich mixtures have higher concentrations of diatomic molecules such as H_2 compared to the products of lean combustion, which have higher concentrations of triatomic molecules such as H_2O. Since the specific heats of diatomic molecules are smaller than those of triatomic molecules, the adiabatic flame temperatures of richer mixtures should have higher values.

As the combustion process in different applications such as diesel or gas turbine cycles can be considered at different pressures, the effect of pressure and initial temperature on the maximum adiabatic flame temperature is also investigated and shown in Figure 8 (right). The results demonstrate that the adiabatic flame temperature of different blends of H_2/NH_3 is weakly affected by pressure so that for a mixture of 50% hydrogen, T_{ad} just increases from 2,224 to 2,242 K as a result of a 20 bar increase in pressure. On the other hand, the effect of initial temperature on the adiabatic flame temperature is more than that of pressure.

4 Conclusions

In this study, thermodynamic analysis of thermal ammonia decomposition to produce hydrogen-rich fuel is performed using Aspen Plus V.12 considering the Gibbs-free energy method. It is found that the performance of the ammonia decomposition reactor is highly affected by temperature and pressure so higher temperatures and lower pressures lead to a higher percentage of the produced hydrogen. The CR of more than 50% occurred at temperatures 427 and 513 K for pressures of 1 and 10 bar respectively. Moreover, the results reveal that the effect of temperature on the enthalpy of the reaction is more pronounced for temperatures lower than 700 K and this endothermic reaction is thermodynamically favourable at temperatures more than 453 K in the forward direction by reaching negative standard Gibbs free energy. Moreover, adiabatic flame temperature analysis shows that increasing the molar percentage of hydrogen from 0 to 50% leads to the increase of maximum adiabatic flame temperature from 2,079 to 2,216 K. The information and results presented in this thermodynamic investigation can serve as a foundation for the optimum design of different parts of ammonia decomposition systems, evaluating the related experimental research, and developing more efficient systems of hydrogen production in different applications such as dual-fuel vehicular engines, maritime, power plants, and industrial furnaces.

Funding information: The project was financed by Chantier Davie Canada Inc., Canada's premier shipbuilder, based on their work in the field of using alternative fuels for the marine industry.

Author contributions: Payam Shafie: conceptualization, methodology, investigation, analysis, writing – original draft, Alain Dechamplain: conceptualization, supervision, analysis, review & editing, Julien Lepine: conceptualization, supervision, analysis, review & editing.

Conflict of interest: The authors state no conflict of interest.

Ethical approval: The conducted research is not related to either human or animal use.

Data availability statement: The data sets generated during and/or analysed during the current study are available from the corresponding author on reasonable request.

References

[1] Sodiq A, Abdollatif Y, Aissa B, Ostovar A, Nassar N, Elnaas M, et al. A review on progress made in direct air capture of CO_2. Environmental Technology and Innovation. Vol. 29. Netherlands: Elsevier B.V; Feb, 2023, doi: 10.1016/j.eti.2022.102991.

[2] Lecture notes in energy 33 energy solutions to combat global warming [Online]. 2022. http://www.springer.com/series/8874.

[3] The role of low-carbon fuels in the clean energy transitions of the power sector; Jun. 10, 2023. Accessed: [Online] https://www.iea.org/reports/the-role-of-low-carbon-fuels-in-the-clean-energy-transitions-of-the-power-sector.

[4] Ibrahim D, Haris I. Renewable hydrogen production. 1st edn. Netherlands: Elsevier; 2022. doi: 10.1016/C2020-0-02435-7.

[5] Madadi Avargani V, Zendehboudi S, Cata Saady NM, Dusseault MB. A comprehensive review on hydrogen production and utilization in North America: Prospects and challenges. Energy Conversion and Management. Vol. 269. UK: Elsevier Ltd; Oct, 2022 doi: 10.1016/j.enconman.2022.115927.

[6] Ojelade OA, Zaman SF. Ammonia decomposition for hydrogen production: a thermodynamic study. Chem Pap. Jan. 2021;75(1):57–65. doi: 10.1007/s11696-020-01278-z.
[7] Potential roles of ammonia in a hydrogen economy a study of issues related to the use ammonia for on-board vehicular hydrogen storage; Jun. 2023 Accessed: [Online]. https://www.energy.gov/eere/fuelcells/downloads/potential-roles-ammonia-hydrogen-economy.
[8] Production capacity of ammonia worldwide from 2018 to 2022, with a forecast for 2026 and 2030; Jul. 2023 Accessed: [Online]. https://www.statista.com/statistics/1065865/ammonia-production-capacity-globally/.
[9] Al-Breiki M, Bicer Y. Comparative cost assessment of sustainable energy carriers produced from natural gas accounting for boil-off gas and social cost of carbon. Energy Rep. Nov. 2020;6:1897–909. doi: 10.1016/j.egyr.2020.07.013.
[10] Schlapbach L, Züttel A. Hydrogen-storage materials for mobile applications; 2001. www.nature.com.
[11] Lhuillier C, Brequigny P, Contino F, Mounaïm-Rousselle C. Experimental study on ammonia/hydrogen/air combustion in spark ignition engine conditions. Fuel. Jun. 2020;269:117448. doi: 10.1016/j.fuel.2020.117448.
[12] Ryu K, Zacharakis-Jutz GE, Kong SC. Performance characteristics of compression-ignition engine using high concentration of ammonia mixed with dimethyl ether. Appl Energy. 2014;113:488–99. doi: 10.1016/j.apenergy.2013.07.065.
[13] Laval A, Hafnia HT, Vestas SG. Ammonfuel-an industrial view of ammonia as a marine fuel. Jun. 2023; [Online]. https://www.alfalaval.com/globalassets/documents/industries/marine-and-transportation/marine/fcm-lff/ammonia-as-fuel/ammonfuel-report-version-09.9-august-3.pdf.
[14] Zhang H, Li G, Long Y, Zhang Z, Wei W, Zhou M, et al. Numerical study on combustion and emission characteristics of a spark-ignition ammonia engine added with hydrogen-rich gas from exhaust-fuel reforming. Fuel. Jan. 2023;332:125939. doi: 10.1016/j.fuel.2022.125939.
[15] Wang W, Herreros JM, Tsolakis A, York APE. Ammonia as hydrogen carrier for transportation; Investigation of the ammonia exhaust gas fuel reforming. Int J Hydrog Energy. Aug. 2013;38(23):9907–17. doi: 10.1016/j.ijhydene.2013.05.144.
[16] Gill SS, Chatha GS, Tsolakis A, Golunski SE, York APE. "Assessing the effects of partially decarbonising a diesel engine by co-fuelling with dissociated ammonia,". Int J Hydrog Energy. Apr. 2012;37(7):6074–83. doi: 10.1016/j.ijhydene.2011.12.137.
[17] Wang B, Yang C, Wang H, Hu D, Wang Y. Effect of diesel-ignited ammonia/hydrogen mixture fuel combustion on engine combustion and emission performance. Fuel. Jan. 2023;331:125865. doi: 10.1016/j.fuel.2022.125865.
[18] Alagharu V, Palanki S, West KN. Analysis of ammonia decomposition reactor to generate hydrogen for fuel cell applications. J Power Sources. Feb. 2010;195(3):829–33. doi: 10.1016/j.jpowsour.2009.08.024.
[19] Lucentini I, Garcia X, Vendrell X, Llorca J. Review of the decomposition of ammonia to generate hydrogen. Ind Eng Chem Res. Dec. 2021;60(51):18560–611. doi: 10.1021/acs.iecr.1c00843.
[20] Chen S, Takata T, Domen K. Particulate photocatalysts for overall water splitting. Nat Rev Mater. Aug. 2017;2(10):17050. doi: 10.1038/natrevmats.2017.50.
[21] Lucentini I, Casanovas A, Llorca J. Catalytic ammonia decomposition for hydrogen production on Ni, Ru and Ni-Ru supported on CeO_2. Int J Hydrog Energy. 2019;44(25):12693–707.
[22] Sittichompoo S, Nozari H, Herreros J, Serhan N, Silva J, York A, et al. Exhaust energy recovery via catalytic ammonia decomposition to hydrogen for low carbon clean vehicles. Fuel. Feb. 2021;285:119111. doi: 10.1016/j.fuel.2020.119111.
[23] Kane SP, Northrop WF. Thermochemical recuperation to enable efficient ammonia-diesel dual-fuel combustion in a compression ignition engine. Energies. Nov. 2021;14(22):7540. doi: 10.3390/en14227540.
[24] Özkara-Aydınoğlu Ş. Thermodynamic equilibrium analysis of combined carbon dioxide reforming with steam reforming of methane to synthesis gas. Int J Hydrog Energy. Dec. 2010;35(23):12821–28. doi: 10.1016/j.ijhydene.2010.08.134.
[25] Çengel YA, Boles MA. Thermodynamics: An engineering approach. 8th edn. McGraw-Hill; 2014.
[26] kenneth KK. Review of chemical thermodynamics. Principles of Combustion. 1st edn. USA: John Wiley & Sons; 1986. p. 6–105.
[27] Abashar MEE. Ultra-clean hydrogen production by ammonia decomposition. J King Saud Univ – Eng Sci. Jan. 2018;30(1):2–11. doi: 10.1016/j.jksues.2016.01.002.
[28] Schmal M, Pinto J. Chemical Reaction Engineering, 2nd ed, Taylor & Francis; 2014.
[29] Franck EU, Cox JD, Wagman DD, Medvedev VA. CODATA — Key values for Thermodynamics, aus der Reihe: CODATA, Series on thermodynamic properties. Hemisphere Publishing Corporation, New York, Washington, Philadelphia, London 1989. 271 seiten, Preis: £ 28.00. Berichte der Bunsengesellschaft für physikalische Chemie. Vol. 94. Issue. 1; Jan 1990. p. 93–3. doi: 10.1002/bbpc.19900940121.
[30] McAllister S, Chen J, Pello A. Fundamentals of combustion processes. Springer; 2012. p. 15–47. doi: 10.1007/978-1-4419-7943-8.
[31] Kurien C, Mittal M. Review on the production and utilization of green ammonia as an alternate fuel in dual-fuel compression ignition engines. Energy Conversion and Management. Vol. 251. Elsevier Ltd; Jan. 2022. doi: 10.1016/j.enconman.2021.114990.
[32] Law CK, Makino A, Lu TF. On the off-stoichiometric peaking of adiabatic flame temperature. Combust Flame. Jun. 2006;145(4):808–19. doi: 10.1016/j.combustflame.2006.01.009.